# Quantum Liang Information Flow as Causation Quantifier

Bin Yi and Sougato Bose
*Department of Physics and Astronomy, University College London, Gower Street, WC1E 6BT London, United Kingdom*

(Received 30 January 2022; accepted 22 June 2022; published 5 July 2022)

Liang information flow is widely used in classical systems and network theory for causality quantification and has been applied widely, for example, to finance, neuroscience, and climate studies. The key part of the theory is to freeze a node of a network to ascertain its causal influence on other nodes. Such a theory is yet to be applied to quantum network dynamics. Here, we generalize the Liang information flow to the quantum domain with respect to von Neumann entropy and exemplify its usage by applying it to a variety of small quantum networks.

DOI: 10.1103/PhysRevLett.129.020501

*Introduction.*—The significance of information flow lies in its logical association [1] with the important notion of causation [2–7]. Historically, various measures of classical information flow were proposed, e.g., Refs. [2,5,7–12]. Nonetheless, limitations were pointed out, e.g., Refs. [11,13,14], the most severe being an incorrect reflection of causality. In 2005, Liang and Kleeman found a law for two-dimensional classical systems [5]. Later on, the dimensionality and determinism limitations were overcome, and eventually Liang was able to link information flow to causality and establish a universally applicable formalism within the framework of classical dynamical systems [1,5,15–18]. This series of works puts the notion of information flow and causation on a rigorous footing, as Liang [1] argued: "Information flow and causality can be derived *ab initio*." The formalism has been validated with various benchmark cases [1] and successfully applied to many realistic problems: glaciology [19], neuroscience [20], El Niño study [16] and prediction [21], precipitation-soil moisture interaction [22], global climate change [23,24], economics [25], etc.

The discussion of causality in quantum physics goes back to the paradigmatic Bell experiment [26]. Causal structure places constraints on the correlations that can be generated in any classical hidden variable theories, which quantum physics violates [27–31]. Motivated by the possible relation between causality and correlations (Liang just put this relation in a mathematical formula [1,16]), various attempts have been made to estimate causal influences in certain quantum environments [32–39]. The quantification of causal effects in the quantum regime sheds new light on quantum communication [40,41] and helps understanding information flow in quantum processors [42,43]. Usually, correlation functions of a Heisenberg picture evolving operators are used to ascertain casual influences, but caution should be exercised, since correlation does not imply causation [1,16].

Surprisingly, the straightforward approach to ascertaining causality that an experimentalist will naturally employ, i.e., to subtract a given component from a network and examine its influence, remains unexplored. Motivated by that, we hereafter adopt Liang's methodology to formulate quantum information flow. As opposed to all the approaches mentioned above in the quantum context, here one detaches or freezes a certain subsystem of a network (sender) in order to ascertain its causal influence on other subsystems (target). The change of a target element's von Neumann entropy, which possesses various interpretations [44], then gives the information flow from the sender.

*Definition.*—Consider a multipartite system with a density operator state $\rho$, evolving under a generic unitary operator $U(t)$. The evolution leads to an entropy change of its subsystems, as initial uncertainties can flow between the subsystems as well as when they get correlated quantum mechanically with each other (an open system is also addressed here by tracing out the ancillary degrees of freedom). Following Liang's methodology (briefly reviewed in Supplemental Material [45]), we decompose the time rate of change of the von Neumann entropy of a subsystem $A$, $dS_A/dt$, into two parts: $T_{B\to A}$, the rate of information flow from subsystem $B$ to $A$, and $(dS_{A\not B}/dt)$, the entropic evolution rate of subsystem $A$ with the influence from $B$ excluded:

$$T_{B\to A} = \frac{dS_A}{dt} - \frac{dS_{A\not B}}{dt}. \tag{1}$$

$S$ is the von Neumann entropy given by $S = -\mathrm{Tr}(\sigma \log \sigma)$ for arbitrary state $\sigma$. $S_{A\not B} = S(\rho_{A\not B}) = S[\varepsilon(t)_{A\not B}\rho_A(0)]$, where $\varepsilon(t)_{A\not B}$ is a map denoting the evolution of $A$ with $B$ frozen. We will discuss the definition and properties of $\varepsilon(t)_{A\not B}$ in the following section. If we consider time evolution as a discrete mapping during interval $\Delta t$, the cumulative information flow is then formulated in terms of the change of entropy $\Delta S$:

 

$$\mathbb{T}_{B\to A} = \int T_{B\to A} dt = \Delta(S_A - S_{A\not B}). \tag{2}$$

Note that the von Neumann entropy, and hence the information flow formalism, possesses various interpretations [44]. Particularly distinct from the Shannon entropy, the von Neumann entropy quantifies the entanglement within a pure bipartite quantum system. $S_{A\not B}$ (or $S_A$) can then be interpreted as the entanglement between $A$ and the rest of the Universe with (or without) $B$ frozen. The term $(S_A - S_{A\not B})$ that appears in Eqs. (1) and (2) is then the difference of these two entanglement measures, in units of ebits. $\mathbb{T}_{B\to A}$ then quantifies the causal influence of $B$ on $A$ in the sense of how much it causes the entanglement of $A$ with the rest of the Universe to change. Similarly, other interpretations, such as the uncertainty of a given state, also apply here.

*Evolution of subsystem A with B frozen.*—Since $\varepsilon(t)_{A\not B}$ is a mapping of states, it can be interpreted as a quantum channel acting on subsystem $A$ [44]: $\rho_A(0) \xrightarrow{\varepsilon(t)_{A\not B}} \rho_{A\not B}(t)$. We further require that $\varepsilon(t)_{A\not B}$ corresponds to a physical process; therefore, it can be obtained from taking the partial trace of the full system, which evolves unitarily. For tripartite system $\rho_{ABC}$,

$$\rho_{A\not B}(t) = \mathrm{Tr}_{BC}\{U_{A\not BC}(t)\rho_{ABC}(0)U^\dagger_{A\not BC}(t)\} \tag{3}$$

for some unitary operator $U_{A\not BC}$.

Moreover, we require that the evolution mechanism with some subsystems frozen takes a product form between the frozen qubits and the rest of the system:

$$U_{A\not BC}(t) = \mathcal{V}_{AC} \otimes \mathcal{W}_B, \tag{4}$$

where $\mathcal{V}_{AC}$ and $\mathcal{W}_B$ are unitary operators acting on subsystems $AC$ and $B$, respectively. The frozen mechanism of the form Eq. (4) guarantees what Liang referred to as *the principle of nil causality* [1] (see Supplemental Material [45] for the proof):

$T_{B\to A} = 0$ *if the evolution of A is independent of B*; *that is, the unitary evolution operator* $U_{ABC}(t)$ *takes separable form* $\mathcal{M}_A \otimes \mathcal{N}_{BC}$ *or* $\mathcal{O}_{AC} \otimes \mathcal{Q}_B$.

Therefore, the causal structure of space-time in physics is embedded in the formalism. If quantum operations, conducted at four-dimensional coordinates $x$ and $y$, are spacelike separated, and hence noncausal, then the operations acting at $x$ do not affect the state located at $y$ and vice versa. The quantum operations at $x$ and $y$ commute, and the joint evolution is in product form. Thus, the quantum Liang information flow from one coordinate to another vanishes.

*Bipartite system.*—Consider a bipartite state $\rho_{AB}$ under unitary evolution $U_{AB}(t)$. Comparing with Eq. (4), $U_{A\not B}$ takes the form $\mathcal{V}_A \otimes \mathcal{W}_B$ in two dimensions. Since von Neumann entropy is invariant under a unitary change of basis, $\rho_{A\not B} = \mathcal{V}_A\rho_A(0)\mathcal{V}_A^\dagger$ and $(dS_{A\not B}/dt) = 0$. Therefore, the rate of information flow from $B$ to $A$: $T_{B\to A} = (dS_A/dt)$. Similarly, $T_{A\to B} = (dS_B/dt)$. If the initial state $\rho_{AB}(0)$ is pure, that is, the system is closed, by Schmidt decomposition, $\rho_A$ and $\rho_B$ share the same set of eigenvalues. Since a closed bipartite system is symmetric, $S_A(t) = S_B(t)$ and $T_{B\to A} = T_{A\to B}$. In general, if the initial state $\rho_{AB}(0)$ is mixed, which can arise from entanglement with some external system, then we no longer have the symmetry $T_{A\to B} \neq T_{B\to A}$. Consider a CNOT gate with controlled qubit $A$ and target qubit $B$ acts on the initial state $\rho_{AB}(0) = (1/2|0\rangle\langle 0|_A + 1/2|1\rangle\langle 1|_A) \otimes |0\rangle\langle 0|_B$; the system evolves to $1/2|0\rangle\langle 0|_A \otimes |0\rangle\langle 0|_B + 1/2|1\rangle\langle 1|_A \otimes |1\rangle\langle 1|_B$. The cumulative information flow for this discrete mapping $\mathbb{T}_{B\to A} = \Delta S_A = 0$ and $\mathbb{T}_{A\to B} = \Delta S_B = 1$ bit. The asymmetric quantum information flow obtained for an initially mixed bipartite system parallels its classical counterpart (see Supplemental Material [45] for details). For multipartite system $\rho_{ABCD\ldots}$, the information flow from the rest of a closed system toward a particular unit, say, $A$, is equivalent to the bipartite scenario: $T_{BCD\ldots\to A} = (dS_A/dt)$, $\mathbb{T}_{BCD\ldots\to A} = \Delta S_A$.

*Multipartite system.*—Evaluation of the information flow in a multipartite system requires a method to fix $\mathcal{V}_{AC}$ in Eq. (4). Here, we demonstrate this with a tripartite system $\rho_{ABC}$. We define the evolution of $A$ with $B$ frozen by replacing the interaction terms relevant to $B$ in the Hamiltonian with the identity operator. For simplicity, consider the evolution operator generated from a time-independent Hamiltonian $H$, $U(t) = e^{-iHt}$, with $\hbar$ set to unity. For instance, let

$$H_{ABC} = H_{0A} + H_{0B} + H_{0C} + \mathcal{A} \otimes \mathcal{C} + \mathcal{B} \otimes \mathcal{C}, \tag{5}$$

where $H_{0i}$, with $i = A, B, C$, is the free Hamiltonian. $\mathcal{A}$, $\mathcal{B}$, and $\mathcal{C}$, which occur in the interactions, are Hermitian operators acting on subsystems $A$, $B$, and $C$, respectively. The evolution mechanism with $B$ frozen is then $U_{A\not BC} = e^{-iH_{A\not BC}t}$, where

$$H_{A\not BC} \equiv H_{0A} + H_{0C} + \mathcal{A} \otimes \mathcal{C} + I_B. \tag{6}$$

$U_{A\not BC}$ is clearly of the product form given in Eq. (4), with $\mathcal{W}_B = I$ and $\mathcal{V}_{AC}$ generated by Hermitian operator $H_{0A} + H_{0C} + \mathcal{A} \otimes \mathcal{C}$. The meaning of $U_{A\not BC}$ is then *evolution of the system if subsystem B is removed from the original evolution mechanism.*

The operational meaning of the frozen mechanism guarantees that this definition is basis (observable) independent. Now, we are equipped with the tools needed to evaluate quantum Liang information flow.

*Application: Multiqubit spin system.*—Consider a multiqubit spin chain. The interaction Hamiltonian between any two interacting qubits $i$ and $j$ is given by [47]

$$H_{\mathrm{spin},ij} = \eta_{ij}(\sigma_{+i}\sigma_{-j} + \sigma_{-i}\sigma_{+j}), \tag{7}$$

where $\sigma_{\pm}$ can be expressed in terms of Pauli matrices $\{\sigma_{x,y,z}\}$, $\sigma_{\pm} = \frac{1}{2}(\sigma_x \pm i\sigma_y)$, and $\eta_{ij}$ represents the coupling strength. The interaction Hamiltonian for three interacting qubits, labeled $A$, $B$, and $C$, of the form Eq. (5) is given by

$$H_{\text{int},ABC} = \eta_{AC}(\sigma_{+A}\sigma_{-C} + \sigma_{-A}\sigma_{+C}) + \eta_{BC}(\sigma_{+B}\sigma_{-C} + \sigma_{-B}\sigma_{+C}). \tag{8}$$

For simplicity, $\eta$ has scaled value with respect to unit relative coupling strength of frequency dimensions. Time $t$ is scaled inversely to unit relative coupling strength.

*Relative coupling strength variation.*—We here investigate the cumulative information flow $\mathbb{T}$ from $A$ and $B$ to $C$ with different coupling strengths; the classical counterpart is seen in Ref. [48]. We set the initial state of the sending qubits $A$ and $B$ being maximally mixed while the receiving qubits $C$ pure: $\rho(0) = I_A \otimes I_B \otimes |0\rangle\langle 0|_C$. So the sending qubits are competing to propagate uncertainty toward the target qubit. The Hamiltonian with one qubit frozen, say, $A$, is obtained by erasing the terms involving qubit $A$ in Hamiltonian Eq. (8):

$$H_{\text{int},\not{A}BC} = \eta_{BC}(\sigma_{+B}\sigma_{-C} + \sigma_{-B}\sigma_{+C}) + I_A. \tag{9}$$

The evolution of $\rho_{\not{A}BC}$ is defined similarly by removing Hermitian terms relevant to qubits $A$ and $B$ altogether. Therefore, $\Delta S_{\not{A}BC}$ vanishes, and the joint cumulative information flow from $AB$ to $C$ is $\mathbb{T}_{AB\to C} = \Delta S_C$. Set $\eta_{AC} = 1$ and $\eta_{BC} = 3$; at time $t \sim 0.49$, the entropy of $C$ reaches its maxima of 1 bit for the first time. This is the maximum uncertainty qubit $C$ can receive, determined by its dimension. For the purpose of illustration, we compare the cumulative information flow from different sending qubits before this capacity is reached. The early time behavior of cumulative information flow $\mathbb{T}_{AB\to C}(t)$, $\mathbb{T}_{A\to C}(t)$, and $\mathbb{T}_{B\to C}(t)$ is plotted in Fig. 1(a).

From Fig. 1(a), we notice that the cumulative information flow from $B$ to $C$ is greater than that from $A$ to $C$: $\mathbb{T}_{B\to C} > \mathbb{T}_{A\to C}$. This formalism is consistent with the intuition that the strongly coupled qubit has greater impact on the target. The direct addition of cumulative information flow from individual qubits $A$ and $B$ is smaller than the joint value: $\mathbb{T}_{B\to C} + \mathbb{T}_{A\to C} < \mathbb{T}_{AB\to C}$ in this example. It means that turning off qubits $A$ and $B$ altogether has more impact on qubit $C$ than the direct addition of turning $A$ and $B$ off one at a time. A similar result is obtained for the early time behavior of a five-qubit spin chain (see Supplemental Material [45]).

*Initial configuration dependence.*—Note that the information flow formalism also depends on the initial configuration. To see how different initial states affect the information flow, set the coupling constant equal: $\eta_{AC} = \eta_{BC} = 1$, with initial state $\rho_{0(1)} = I_A \otimes (0.9|0\rangle\langle 0| + 0.1|1\rangle\langle 1|)_B \otimes |0\rangle\langle 0|_C$ and $\rho_{0(2)} = I_A \otimes (0.1|0\rangle\langle 0| + 0.9|1\rangle\langle 1|)_B \otimes |0\rangle\langle 0|_C$.

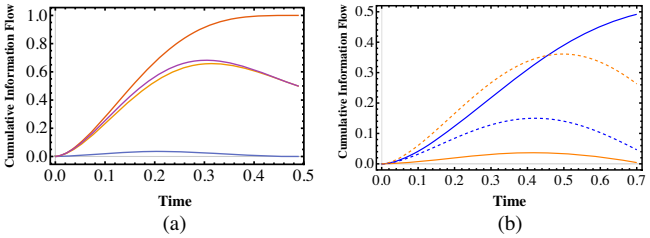


FIG. 1. Three-qubit spin chain. (a) From top to bottom (measured in bits): $\mathbb{T}_{AB\to C}$, $\mathbb{T}_{B\to C} + \mathbb{T}_{A\to C}$, $\mathbb{T}_{B\to C}$, and $\mathbb{T}_{A\to C}$. Coupling strength: $\eta_{AC} = 1$, $\eta_{BC} = 3$. Initial state: $\rho(0) = I_A \otimes I_B \otimes |0\rangle\langle 0|_C$. (b) Blue curves, $\mathbb{T}_{A\to C}$; orange curves, $\mathbb{T}_{B\to C}$. Solid curves, initial state $\rho_{0(1)} = I_A \otimes (0.9|0\rangle\langle 0| + 0.1|1\rangle\langle 1|)_B \otimes |0\rangle\langle 0|_C$; dashed curves, initial state $\rho_{0(2)} = I_A \otimes (0.1|0\rangle\langle 0| + 0.9|1\rangle\langle 1|)_B \otimes |0\rangle\langle 0|_C$. Coupling strength $\eta_{AC} = \eta_{BC} = 1$.

In both cases, the initial entropy of qubit $B$ is ~0.47 bit, while $A$ is 1 bit. At first glance, one may be expecting that $A$ is transmitting more uncertainty to $C$ than qubit $B$. From Fig. 1(b), we see this is indeed the case for initial state $\rho_{0(1)}$. But when the initial state is switched to $\rho_{0(2)}$, we have $\mathbb{T}_{B\to C} > \mathbb{T}_{A\to C}$. This is because increasing the von Neumann entropy could result from not only classical uncertainty propagation, but also from entanglement generation. The qubit interaction given in Eq. (7) entangles state $|10\rangle$ ($|01\rangle$), while it does not act on state $|00\rangle$ ($|11\rangle$):

$$(\sigma_+\sigma_- + \sigma_-\sigma_+)|00\rangle = 0, \quad (\sigma_+\sigma_- + \sigma_-\sigma_+)|10\rangle = |01\rangle.$$

For initial state $\rho_{0(2)}$, qubits $B$ and $C$ have 90% probability in the $|10\rangle_{BC}$ state; the entangling mechanism greatly increases $\mathbb{T}_{B\to C}$ compared to $\rho_{0(1)}$, for which the probability is only 10%. Changing the initial state to $\rho_{0(2)}$ also suppresses $\mathbb{T}_{A\to C}$ due to the growing competition from $B$.

*Quantum superexchange.*—Add a constant magnetic field along the $z$ axis with strength $\mathbf{B}$ on the intermediate qubit $C$ so that its energy is lifted by an amount $\mathbf{B}\sigma_z$, while qubits $A$ and $B$ remain unaffected. The total Hamiltonian acting on the system then gains an additional term:

$$H_{\text{additional}} = I_A \otimes I_B \otimes \mathbf{B}\sigma_{z(C)}. \tag{10}$$

Set coupling strength $\eta_{AC} = \eta_{BC} = 1$ and initial state $\rho(0) = I_A \otimes |0\rangle\langle 0|_B \otimes I_C$. We wish to compare information flow from $A$ and $C$ to $B$ with various magnetic field strengths. Note that, when $\mathbf{B} = 0$, the dynamics of information flow in the $XY$ model [Eq. (7)], which is not *a priori* obvious, can be pictured from Fig. 2(a). The cumulative information flow is initially from $C$ to $B$, and it reaches a high value of 1 bit before it declines and is overtaken by the cumulative information flow from $A$ to $B$. As the magnetic field strength increases, the superexchange process [49] between $A$ and $B$ becomes progressively dominant. Thus, we see that information flow from $C$ to $B$ goes down, while

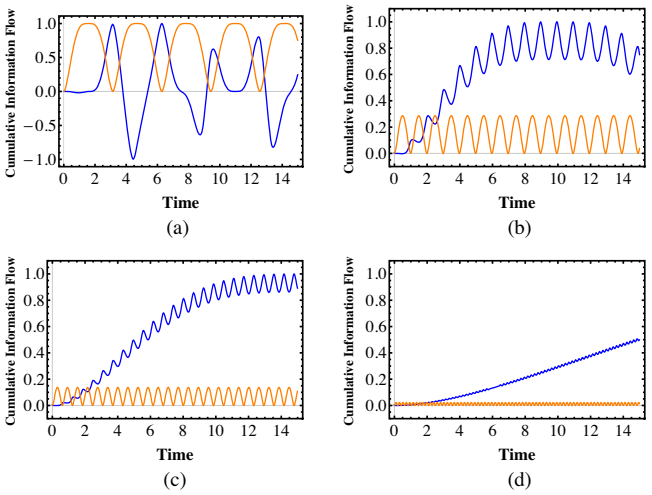


FIG. 2. Quantum superexchange (in bits). Blue curves, $\mathbb{T}_{A\to B}$; orange curves, $\mathbb{T}_{C\to B}$. In (a)–(d), magnetic field strength is set to $\mathbf{B} = 0, 3, 5, 15$, respectively. Coupling strength $\eta_{AC} = \eta_{BC} = 1$. Initial state $I_A \otimes |0\rangle\langle 0|_B \otimes I_C$.

that from $A$ to $B$ becomes that dictated by an effective weaker superexchange coupling $\eta_{AC}^2/\mathbf{B}$ between $A$ and $B$ $(\sigma_{+A}\sigma_{-B} + \text{H.c.})$ [49].

*Five-qubit network.*—Consider a five-qubit spin system, labeled $A$, $B$, $C$, $D$, $E$, with $E$ in the center; we wish to investigate the information flow toward $E$. The total Hamiltonian for the five-qubit spin chain is

$$H_{\text{spin,tot}} = \sum_i H_{\text{spin},iE} \tag{11}$$

with $i = A, B, C, D$. Set all the coupling strengths with $E$ identical: $\eta_{\text{DE}} = \eta_{CE} = \eta_{BE} = \eta_{AE} = 1$, and initial state of sending qubits $A$, $B$, $C$, and $D$ maximally mixed, receiving qubit $E$ pure. At time $t \sim 0.69$, the entropy of $E$ reaches its maximum of 1 bit for the first time. The cumulative information flow from each sending qubit, which is identical $\mathbb{T}_{A\to E} = \mathbb{T}_{B\to E} = \mathbb{T}_{C\to E} = \mathbb{T}_{D\to E}$, is plotted for the time interval $t \in [0, 0.69]$ in Fig. 3(a).

Now let us add mutual interaction between $C$ and $D$ with a relative coupling strength $\eta_{CD} = 5$ and observe how the information flow toward the central qubit $E$ changes (a schematic diagram of the interaction pattern is shown in Supplemental Material [45]). The total Hamiltonian is now given by

$$\sum_i H_{\text{spin},iE} + H_{\text{spin},CD}. \tag{12}$$

With this additional interaction term, the cumulative information flow from each sending qubit to $E$ is plotted in Fig. 3(b). Comparing Figs. 3(b) to 3(a), the additional interaction term between $C$ and $D$ greatly reduces the transmitted uncertainty from qubit $C$ $(D)$ to qubit $E$ while

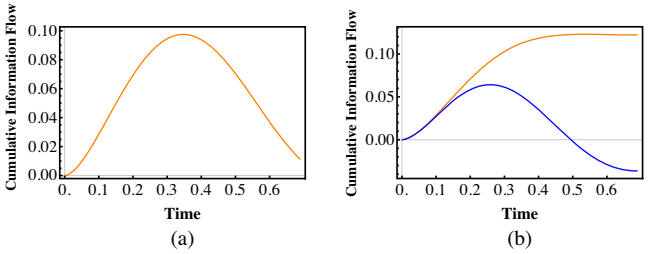


FIG. 3. Five-qubit network. Cumulative information flow (in bits). (a) From any sending qubit toward $E$ with identical coupling strength: $\eta_{\text{DE}} = \eta_{CE} = \eta_{BE} = \eta_{AE} = 1$. (b) With additional coupling $\eta_{CD} = 5$. Orange curve, $A$ (or $B$) to $E$; blue curve, $C$ (or $D$) to $E$.

increasing that from qubit $A$ $(B)$ to qubit $E$. After time $t \sim 0.49$, $\mathbb{T}_{C\to E}$ reaches a negative value; that is, the presence of qubit $C$ $(D)$ reduces the uncertainty of qubit $E$. The uncertainty from qubit $C$ $(D)$ now has two routes to propagate, toward either $E$ or $D$ $(C)$. Also, the relative coupling strength $\eta_{CD}$ is 5 times stronger than $\eta_{CE}$ and $\eta_{\text{DE}}$. The strongly coupled route connecting $C$ and $D$ then diverts the uncertainty propagation away from the original path between $C$ $(D)$ and $E$, so that $\mathbb{T}_{C\to E}$ $(\mathbb{T}_{D\to E})$ decrease. Qubits $A$ and $B$ now have less competition from qubits $C$ and $D$ to propagate uncertainty toward qubit $E$. Then, $\mathbb{T}_{A\to E}$ $(\mathbb{T}_{B\to E})$ increases. The presence of certain coupling can, thus, be used to preserve information. Although beyond the scope of this proof of principle work, we point out that this methodology could be exploited to design robust quantum circuits. Take variational quantum algorithms on noisy intermediate-scale quantum computers, for instance [50]. The parameters of a quantum circuit are optimized to give a minimum cost function. Ground state energy is typically the choice of cost function in many cases (e.g., solving quantum many-body systems). One can add to this the average quantum Liang information flow, for instance, from one node to another as a supplementary cost function. In that case, the optimized circuit will be more robust against single-node failure.

*Application: Two-qubit system in bosonic bath.*—Let $A$ and $B$ indicate two noninteracting qubits with ground and excited states $|0\rangle$ and $|1\rangle$, embedded in a common zero-temperature bosonic reservoir labeled $C$. We wish to compare the information flow between the two qubits. The Hamiltonian governing the mechanism is given by $H_{SB} = H_0 + H_{\text{int}}$, with

$$\begin{aligned} H_0 &= \omega_0\sigma_+^A\sigma_-^A + \omega_0\sigma_+^B\sigma_-^B + \sum_k \omega_k b_k^\dagger b_k, \\ H_{\text{int}} &= \alpha_A\sigma_+^A\sum_k g_k b_k + \alpha_B\sigma_+^B\sum_k g_k b_k + \text{H.c.}, \end{aligned} \tag{13}$$

where $\sigma_\pm^{A(B)}$ and $\omega_0$ are the inversion operator and transition frequency of qubit $A$ $(B)$, respectively. $b_k$ and $b_k^\dagger$ are the

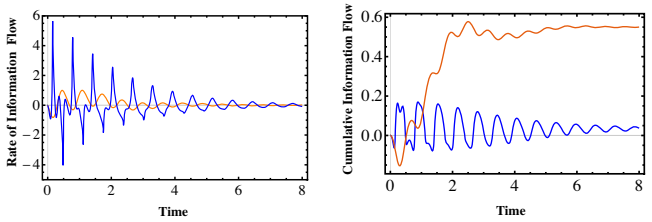


(a) (b)

FIG. 4. Two-qubit system in a lossy cavity. Blue curves: from $B$ to $A$. Orange curves: from $A$ to $B$. Coupling strength ratio $\alpha_A/\alpha_B = 10/1$. (a) Rate of information flow (bits per unit time). (b) Cumulative information flow (bits).

annihilation and creation operator, respectively, of the environment $C$. $\alpha_{A(B)}$ measures the coupling between each qubit and the reservoir. In the limit $\alpha_B$ or $\alpha_A$ goes to 0, that is, when one of the qubit decouples from the setup, then $\rho_A$ and $\rho_{AB}$ obeys the same equation of motion and $\rho_A(t) = \rho_{AB}(t)$. Therefore, $T_{B\to A} = T_{A\to B} = 0$.

We adopt the lossy cavity model given in Ref. [51]. The two-qubit dynamics is solved exactly at zero temperature. Take initial state $\rho_{AB}(0) = |\psi_0\rangle\langle\psi_0|$, where $|\psi_0\rangle = (1/\sqrt{3})(|01\rangle + \sqrt{2}|10\rangle)$. Set $\lambda$ and $\hbar$ equal to unity, $\alpha_A/\alpha_B = 10/1$, and take strong coupling limit $R = 10$, where $\lambda$ defines the spectral width of the coupling and $R$ determines the collective coupling strength. The rate of information flow with respect to scaled time $t$ from $B$ to $A$ versus that from $A$ to $B$ is plotted in Fig. 4(a). The cumulative information flow is shown in Fig. 4(b). From Fig. 4(a), we see that the rate of information flow from the weakly coupled qubit ($B$) toward the strongly coupled qubit ($A$) possesses a higher peak than that from $A$ to $B$. On the other hand, as shown in Fig. 4(b), the cumulative information flow from $A$ to $B$ grows steadily and surpasses that from $B$ to $A$ as the system approaches equilibrium. Note that the information flow formalism is generically asymmetric $T_{\to A} \neq T_{A\to B}$, as opposed to most quantum correlation measures.

*Conclusions.*—We have generalized Liang's theory and methodology for classical systems to quantify causality in quantum networks. A unique feature of quantum networks is the possibility of entanglement. Thus, there are two ways to increase the entropy of a node: (i) classical uncertainty propagation and (ii) growth of entanglement. It is found that the information flow between two qubits through a common bath could be nontrivial: The weakly coupled qubit has a higher rate of information flow, while, in the long run, the strongly coupled qubit has more impact. Another nontrivial result obtained for a five-qubit network reveals that an additional strong coupling diverts the directions of uncertainty propagation. The information-flow-based causal measure may have applications in parallel with its classical counterparts [1,16–20,22,23,52,53].

B. Y. thanks S. X. Huang for introducing the problem and A. J. Leggett and X. S. Liang for inspiring discussions. S. B. acknowledges the Engineering and Physical Sciences Research Council grant nonergodic quantum manipulation No. EP/R029075/1.

[1] X. S. Liang, Phys. Rev. E **94**, 052201 (2016).
[2] C. Granger Investigating casual relations by econometric models and cross spectral (1969).
[3] J. Pearl *et al. Models, Reasoning and Inference* (Cambridge University Press, Cambridge, England, 2000), Vol. 19.2.
[4] P. Spirtes, C. N. Glymour, R. Scheines, and D. Heckerman, *Causation, Prediction, and Search* (MIT Press, Cambridge, MA, 2000).
[5] X. S. Liang and R. Kleeman, Phys. Rev. Lett. **95**, 244101 (2005).
[6] B. P. Bezruchko and D. A. Smirnov, *Extracting Knowledge from Time Series: An Introduction to Nonlinear Empirical Modeling* (Springer Science & Business Media, New York, 2010).
[7] T. Schreiber, Phys. Rev. Lett. **85**, 461 (2000).
[8] J. A. Vastano and H. L. Swinney, Phys. Rev. Lett. **60**, 1773 (1988).
[9] D. W. Bunn and C. Fezzi Interaction of European carbon trading and energy prices (2007).
[10] M. Staniek and K. Lehnertz, Phys. Rev. Lett. **100**, 158101 (2008).
[11] J. Sun and E. M. Bollt, Physica (Amsterdam) **267D**, 49 (2014).
[12] C. Cafaro, W. M. Lord, J. Sun, and E. M. Bollt, Chaos **25**, 043106 (2015).
[13] D. W. Hahs and S. D. Pethel, Phys. Rev. Lett. **107**, 128701 (2011).
[14] D. A. Smirnov, Phys. Rev. E **87**, 042917 (2013).
[15] X. S. Liang, Phys. Rev. E **78**, 031113 (2008).
[16] X. S. Liang, Phys. Rev. E **90**, 052150 (2014).
[17] X. S. Liang, Chaos **31**, 093123 (2021).
[18] X. S. Liang, Entropy **23**, 679 (2021).
[19] S. Vannitsem, Q. Dalaiden, and H. Goosse, Geophys. Res. Lett. **46**, 12125 (2019).
[20] D. T. Hristopulos, A. Babul, S. Babul, L. R. Brucar, and N. Virji-Babul, Front. Hum. Neurosci. **13**, 419 (2019).
[21] X. S. Liang, F. Xu, Y. Rong, R. Zhang, X. Tang, and F. Zhang, Sci. Rep. **11**, 1 (2021).
[22] D. F. T. Hagan, G. Wang, X. S. Liang, and H. A. Dolman, J. Climate **32**, 7521 (2019).
[23] A. Stips, D. Macias, C. Coughlan, E. Garcia-Gorriz, and X. S. Liang, Sci. Rep. **6**, 21691 (2016).
[24] D. Docquier, S. Vannitsem, F. Ragone, K. Wyser, and X. S. Liang The rate of information transfer as a measure of rapid changes in Arctic Sea ice (2021).
[25] X. Lu, K. Liu, K. K. Lai, and H. Cui, Procedia Comput. Sci. **199**, 1327 (2022).
[26] J. S. Bell, Phys. Phys. Fiz. **1**, 195 (1964).
[27] S. J. Freedman and J. F. Clauser, Phys. Rev. Lett. **28**, 938 (1972).
[28] A. Aspect, P. Grangier, and G. Roger, Phys. Rev. Lett. **49**, 91 (1982).

[29] B. G. Christensen, K. T. McCusker, J. B. Altepeter, B. Calkins, T. Gerrits, A. E. Lita, A. Miller, L. K. Shalm, Y. Zhang, S. W. Nam *et al.*, Phys. Rev. Lett. **111**, 130406 (2013).
[30] M. A. Rowe, D. Kielpinski, V. Meyer, C. A. Sackett, W. M. Itano, C. Monroe, and D. J. Wineland, Nature (London) **409**, 791 (2001).
[31] M. Giustina, A. Mech, S. Ramelow, B. Wittmann, J. Kofler, J. Beyer, A. Lita, B. Calkins, T. Gerrits, S. W. Nam *et al.*, Nature (London) **497**, 227 (2013).
[32] M. Gachechiladze, N. Miklin, and R. Chaves, Phys. Rev. Lett. **125**, 230401 (2020).
[33] J. Henson, R. Lal, and M. F. Pusey, New J. Phys. **16**, 113043 (2014).
[34] R. Chaves, C. Majenz, and D. Gross, Nat. Commun. **6**, 5766 (2015).
[35] F. Costa and S. Shrapnel, New J. Phys. **18**, 063032 (2016).
[36] T. Fritz, Commun. Math. Phys. **341**, 391 (2016).
[37] J. Barrett, R. Lorenz, and O. Oreshkov, arXiv:1906.10726.
[38] E. Wolfe, A. Pozas-Kerstjens, M. Grinberg, D. Rosset, A. Acín, and M. Navascués, Phys. Rev. X **11**, 021043 (2021).
[39] J. Åberg, R. Nery, C. Duarte, and R. Chaves, Phys. Rev. Lett. **125**, 110505 (2020).
[40] J. F. Fitzsimons, J. A. Jones, and V. Vedral, Sci. Rep. **5**, 1 (2015).
[41] R. Pisarczyk, Z. Zhao, Y. Ouyang, V. Vedral, and J. F. Fitzsimons, Phys. Rev. Lett. **123**, 150502 (2019).
[42] C. Di Franco, M. Paternostro, G. M. Palma, and M. S. Kim, Phys. Rev. A **76**, 042316 (2007).
[43] C. Di Franco, M. Paternostro, and G. Palma, Int. J. Quantum. Inform. **06**, 659 (2008).
[44] M. A. Nielsen and I. Chuang, *Quantum Computation and Quantum Information* (Cambridge University Press, New York, USA 2002), pp. 558–559.
[45] See Supplemental Material at http://link.aps.org/supplemental/10.1103/PhysRevLett.129.020501 for a brief review of the Liang-Kleeman analysis and further clarifications on its quantum generalization, which contains Ref. [46].
[46] S. H. Strogatz, Nature (London) **410**, 268 (2001).
[47] M.-H. Yung, D. W. Leung, and S. Bose, Quantum Inf. Comput. **4**, 174 (2004).
[48] X. S. Liang, Entropy **24**, 3 (2021).
[49] S. C. Benjamin and S. Bose, Phys. Rev. A **70**, 032314 (2004).
[50] J. R. McClean, J. Romero, R. Babbush, and A. Aspuru-Guzik, New J. Phys. **18**, 023023 (2016).
[51] R. L. Franco, B. Bellomo, S. Maniscalco, and G. Compagno, Int. J. Mod. Phys. B **27**, 1345053 (2013).
[52] C. Cafaro, S. A. Ali, and A. Giffin, Phys. Rev. E **93**, 022114 (2016).
[53] J. M. Horowitz and M. Esposito, Phys. Rev. X **4**, 031015 (2014).